

Accepted for publication in *the ApJ* August 1, 2003

A Method for Black Hole Mass Determination in Accretion Powered X-Ray Sources

Chris R. Shrader^{1,3}, & Lev Titarchuk^{1,2,4}

ABSTRACT

We describe a method for the determination of black-hole masses based on information inferred from high-energy spectra. It is required that the spectral energy distribution consist of thermal and Comptonized components. One can then, in principle, infer the depth of the gravitational potential well for sources of known distance. The thermal component is inferred by the integration of a blackbody spectral form over the disk. We assume that the color temperature distribution in the disk has a specific shape given by the Shakura-Sunyaev (1973) disk model which goes to zero at the inner disk radius and at infinity and has a maximum at 4.2 Schwarzschild radii. In this formulation there is only one parameter, the so called color correction factor, relating the apparent temperature to effective temperature which characterizes the thermal emission component. We have made use of improved Galactic black hole binary dynamical mass determinations to derive, in effect, an empirical calibration of this factor. We then present our analysis of observational data for representative objects of several classes; Galactic black hole X-ray binaries, narrow line Seyfert galaxies (NLS1), and “ultra-luminous” extragalactic X-ray sources (ULX). We then apply our mass determination calculation and present our results. We argue that this approach can potentially fill a void in the current knowledge of NLS1 and ULX properties, and discuss how a deeper understanding of both classes has relevance to the broader issues of how cosmic black holes, beyond the stellar-mass realm, are formed and what is their overall mass distribution.

¹Laboratory for High Energy Astrophysics, NASA Goddard Space Flight Center, Greenbelt, MD 20771, USA; Chris.R.Shrader@gsfc.nasa.gov, titarchuk@lheapop.gsfc.nasa.gov

²E.O. Hulbert Center for Space Research, Naval Research Laboratory

³Universities Space Research Association, Lanham MD

⁴George Mason University/CEOSR, Fairfax VA

Subject headings: accretion — black hole physics — radiation mechanisms: non-thermal — relativity — galaxies:active — galaxies:nuclei — galaxies:Seyfert — quasars:general

1. Introduction

Recent developments leading to renewed interest in the problem of the cosmic distribution of black hole masses, their origin and growth, have motivated us to propose a new method for black hole mass estimation. In galaxies, the bulge $M - \sigma$ relation, its apparent cross-calibration with reverberation mapping methods and related correlations have provided a greatly expanded database of central black hole masses, and support the idea that masses $\sim (10^6 - 10^7)M_\odot$ are a ubiquitous feature of galaxies (e.g. Ferrarese & Merrit 2000; Wandel, Peterson & Malkan 1999; Woo & Urry 2002). However, velocity dispersion data are difficult to obtain for a large sample of objects, the reverberation mapping efforts are observationally intensive to compile and the correlation methods potentially suffer from calibration uncertainty. In a number of external galaxies, notably ones with active star formation regions, the so called "Ultra-luminous" X-ray sources (ULXs) have led to speculation on the existence of intermediate $(10^2 - 10^4)M_\odot$ mass objects [e.g. Colbert & Mushotzky 1999; Strohmayer & Mushotzky 2003; Miller et al 2003]. However, the prospects for dynamical measurement supporting these assertions are poor.

In parallel with these observational developments, a growing inventory of dynamically determined Galactic black hole masses in accretion powered X-ray binaries (herein BHXRBs) continues to emerge (e.g. Orosz 2002). We would thus suggest that pursuit of an independent methodology for BH mass determination is desirable, in particular, one which can be calibrated through use of this knowledge base. The method we propose makes use of the high-energy spectra of these objects. Our work builds upon Borozdin et al. (1999) hereafter BOR99, and Shrader & Titarchuk (1999) hereafter ShT99, where we introduced our basic methodology [also refer to Colbert & Mushotzky (1999), in which one of us (LT), contributed calculations leading to one of the earliest claims of intermediate black hole (IMBH) existence]. The major differences here are that the a greater number of the Galactic binaries are dynamically constrained and can thus be used to test our results, and that we have applied the analysis to representative objects of the ULX and NLS1 classes. We also present some additional computational details and expanded discussion that were absent in the earlier papers.

We further explore possible links to studies of the aforementioned extra-galactic populations. The basis for this extrapolation is the similarity between the X-ray spectra of

a subclass of active galaxies, the narrow-lined Seyferts (NLS1s) and the galactic black-hole binaries. Indeed, it is now apparent that at least some ULXs most likely are accretion driven compact objects (Strohmayer & Mushotzky 2003), and in at least a few cases exhibit the well known bi-modal spectral behavior seen in galactic objects.

The emergent X-ray spectrum of an accretion driven compact source is generally a convolution of a thermal source component associated with an accretion disk flow and the scattering Green’s function which represents the effects of Comptonization by energetic electrons. A deconvolution of these two effects, in principle, allows one to derive with minimal model dependence a physical normalization term for the thermal component from which a distance-to-mass ratio can then be determined. This is the basic idea underlying our method. One particular spectral model is the bulk-motion Comptonization (BMC) model (Titarchuk, Mastichiadis & Kylafis 1996, 1997; Laurent & Titarchuk 1999, 2001), which has already been applied to this problem by Shrader & Titarchuk (1998), hereafter ShT98 and ShT99. However, most of what we discuss here is independent of the particular geometrical and dynamical configuration of the Comptonizing medium. The minimal assumption is required in constructing the multicolor disk spectrum is that the release of gravitational energy of the matter in the disk, presumably due to viscosity, diminishes toward the inner disk boundary. Novikov & Thorne (1973) were the first to formulate this boundary condition [see also Shakura & Sunyaev (1973), hereafter SS73, for detail of the disk structure]. Combination of the viscous dissipation of the gravitational energy and this boundary condition leads to the formation of the color temperature distribution over the disk with a characteristic maximum at about 4.2 Schwarzschild radii (SS73). We note that we do not consider the case of extreme Kerr geometries; further discussion of this issue is presented in section 4.

We assume that the color temperature distribution in the disk has a specific shape, given by the SS73 disk model, which goes to zero at the inner disk radius and at infinity and has a maximum at $R_{max} = 4.2R_S$ where $R_S = 2GM/c^2$ is Schwarzschild radius. This formulation of the disk spectral model, obtained by integration of blackbody spectra over the disk, has only one parameter; the so called color correction factor T_h . The color correction factor relates the apparent temperature $T = T_{col}$ to effective temperature T_{eff} which characterizes the thermal emission component. The color factor $T_h = 2.6$ was calibrated using the spectral measurements of GRO J1655-40 for which the distance and mass of the central objects are known accurately (BOR99).

We note that BOR99 also estimated the central object mass in GRS 1915+105, $m = M/M_\odot = (13.5 \pm 1.5)/(\cos i)^{1/2}$ with an assumption that the same color factor $T_h = 2.6$ is valid for the disk in this source. Recent dynamical measurements of Greiner et al. (2000), who find a mass of 14 ± 4 in GRS 1915+105, further corroborate our results. We were thus en-

couraged to undertake an effort to expand our study of galactic binaries, to further calibrate and, hopefully, validate our method. We then apply the same methods to selected objects among the aforementioned extra- galactic classes for which the high/soft state spectral form is observed.

In this paper, we present the details of our mass-determination method (§ 2), and then proceed to apply our analysis to observational data (§ 3). This includes samples of additional galactic X-ray binaries, NLS1s and several ultra-luminous X-ray sources in nearby galaxies. Comparison to independent mass determinations, and the implications of some of our results are discussed in § 3 and we summarize and draw conclusions in § 4.

2. Description of Mass Determination Method

To summarize the idea of our method we enumerate the main points: (i) We extract as accurately as possible the soft component from the data using the exact form of the Comptonized spectrum derived in Sunyaev & Titarchuk (1980); Titarchuk (1994), Titarchuk & Zannias (1998). (ii) We calibrated the color hardening factor $T_h = T/T_{eff}$ using the GRO J1655-40 for which the distance and the mass are known. We argue that this approach is superior to model-dependent methods (e.g. Shimura & Takahara 1995) given the number of unconstrained free parameters. We note that Merloni Fabian & Ross (2000) and also Hubeny et al. (2001) demonstrate the wide range of possible model-specific T_h values. (iii) When T_h is established, one can proceed with mass determination using the color temperature T and the absolute normalization of the soft component A_n which depends on the mass, distance, inclination angle i and the effective emission area radius r_{eff} that in turn depends on T only (see BOR99, Eqs 4 and 6) allowing us to infer distance-to-mass ratio with an accuracy of $\cos^{1/2}i$. (iv) Our model (using SS73, see details in BOR99) then allows for determination of the effective area, from the observationally determined color temperature T .

In Figure 1 we present an artistic conception of our model. The low-energy blackbody X-ray photons associated with accretion powered objects such as BHXRBS, NLS1s or ULXs, are assumed to come directly from the thin accretion disk, as is well established to be the case in BHXRBS. The higher energy photons that form the power law tail of the spectrum come from upscattering (acceleration) by energetic electrons rushing towards the central black hole. The plasma dynamics is a mixture of thermal and bulk motion inflow. Some part of the disk soft photon flux comes directly to the Earth observer but some fraction of the disk flux Q_d comes after the scattering in the corona region (the site of the energetic particles). In fact, the corona could be very hot if the disk illumination flux Q_d is much less than the energy release in the corona Q_{cor} and it can be relatively cold if $Q_d \gtrsim Q_{cor}$ (see

more details of these picture in Chakrabarti & Titarchuk 1995).

To determine the central object mass, the basic idea is to extract the blackbody component from the emergent spectrum whose shape is modified by Compton scattering off the hot electrons. The intensity of the blackbody radiation we measure depends on the emission area of the accretion disk and the distance to the source, which for extragalactic objects is usually known with reasonable precision. Depending on the color temperature, typically $kT \simeq 1$ keV for BHXRBs, the effective radius associated with this area can be 5-15 Schwarzschild radii.

The next problem is to determine a ratio of color to effective temperature, the so-called color factor, T_h . This characterizes the deviation between the emergent spectrum and a pure blackbody. For the pure blackbody case, the luminosity per unit area is a product of the fourth power of the temperature and the Stefan-Boltzmann constant; this is easily generalized to the multi-temperature disk scenarios. Equating the observed, integrated luminosity to this expression yields a different temperature from that inferred from a spectral fitting procedure using a Planck distribution. This phenomenon is well known in solar and stellar astrophysics. For example, the Sun has an effective temperature of 5500 K, but its spectrum is not described by a 5500-K black body. Physically, this difference results from scattering effects in the solar atmosphere, through which we view the substrata to about an optical depth. In the case of galactic BHXRBs, the appropriate color factor can be determined theoretically by invoking several assumptions regarding the accretion disk, or it can be empirically calibrated using a source for which the black hole mass and distance are already known through independent methods. One must then assume that the color factor inferred is invariant to a reasonable approximation (see more discussion of this issue in §3).

As noted, BOR99 previously calibrated the color factor using a particular source, GRO J1655-40, for which accurate mass, distance and orbital inclination measurements have been made (Orosz & Bailyn 1997; Orosz 2002). The color factor thus obtained was $T_h \simeq 2.6$. We can now expand upon that effort, making use of the additional dynamical binary solutions which have emerged. Once established, T_h can be used along with inferred spectral parameters in a distance-to-mass determination. For Galactic sources, distances are often crudely determined, but in external galaxies they are more precise. A major question which we must address however, is whether or not the color factor is similar for other classes of objects, which are in different environments and different regimes of M and \dot{M} .

2.1. Color Factor Calibration

We have made use of a growing database of dynamically constrained black-hole masses in Galactic binaries (e.g. Orosz 2002) to better calibrate this key parameter of our method; the color correction or "hardening" factor. In BOR99 and ShT99 details of the BH mass determination procedure were presented. For completeness, we duplicate some description of that procedure for the determination of the m/d -ratio here, augmented with some additional details, and arguments supporting its generalization to other object classes.

The inferred absolute normalization of the disk multicolor disk, presented in approximation of as a single blackbody spectrum reads as follows

$$A_N = C_N r_{eff}^2 = \frac{0.91 m^2 \cos i T_h^{-4}}{d^2} r_{eff}^2(T_{col}), \quad (1)$$

where d is the distance to source in kiloparsecs, $\cos i$ is the cosine of the inclination angle (the angle between the line of sight and the normal to the disk) and $r_{eff}(T_{col})$ is the effective radius of the area related to the best-fit blackbody color temperature T_{col} . The blackbody spectral shape with color temperature T_{col} provides a reasonable approximation to the multicolor disk spectrum (e.g. BOR99, eq. [2]) if the ratio of energies (for a given photon energy band) to the best-fit color temperature is greater than 2 (see BOR99, Fig.4). It is worth pointing out the values of the best-fit parameter T_{col} of the observed spectrum and our best-fit parameters r_{eff} and T_{col} are sensitive to the energy range of a given instrument. One should be very careful to take this into account when applying our technique (see details in BOR99 and ShT99)

In the Bulk Motion Comptonization model (BMC) the absolute normalization of the blackbody component \tilde{A}_N is related to A_N :

$$A_N = \frac{8.0525 \tilde{A}_N^{bb}}{(1+f)[kT/(1\text{keV})]^4} \quad (2)$$

where f is the so-called illumination parameter, which for the Comptonized component is

$$A_N^{comp} = A_N^{bb} f / (1+f). \quad (3)$$

In a case of $f \ll 1$ the Compton cloud (presumably in the high/soft state it is the converging inflow) occupies relatively small area, characterized by typically less than 3 Schwarzschild radii and a predominantly thermal spectrum is observed. By comparison, the effective disk area, characterized by $r_{eff} = R_{eff}/R_S$, was found to be more than 10 by Borozdin et al. (1999).

There are cases when $f \gg 1$, for example, during the low/hard state. This indicates that the Compton cloud completely covers the effective disk area. In this case we can also

determine A_N using eq. (2). To do this one can also use \tilde{A}_N^{bb} because $\tilde{A}_N^{comp} = \tilde{A}_N^{bb}f/(1+f) \sim \tilde{A}_N^{bb}$.

In BOR99 we inferred the hardening factor $T_h = 2.6 \pm 0.1$ for GRO J1655-40 using formula (1) in which there was only one unknown parameter, T_h . Specifically, we use $m = 7 \pm 1$, $i = 70^\circ$ (Orosz & Bailyn 1997), $d = 3.2 \pm 0.2$ (Hjellming & Rupen 1995). The effective radius r_{eff} as a function of the best-fit color temperature was calculated (for RXTE data see Fig. 5 in BOR99 and formulas in ShT99). The inferred coefficient A_N was obtained using the best-fit parameters of the BMC model, namely \tilde{A}_N^{bb} , T_{col} and f (see formula 2).

3. Application to Observational Data

We obtained data from the NASA High Energy Astrophysics Science Research Center (HEASARC) for representative samples of BHXRBs, NLS1s, and a few ULX sources. The database utilized for the BHXRB analysis was primarily derived from the the Rossi X-ray Timing Explorer (RXTE) archive, although in several cases this was supplemented with higher energy data from the Compton Gamma Ray Observatory. We used archival data from the ASCA X-ray satellite for most of the NLS1s in our sample, supplemented by publicly available Chandra data for the "type-I" quasar PHL 1811. For the ULXs, we used our spectroscopic analysis was based on ASCA CCD and gas-scintillator spectra (NGC 1313, NGC 5408 and M33), and on Chandra ACIS CCD spectra (NGC 253, NGC 1399 X-2 and X-4). In addition, we examined Chandra images of the ASCA fields to assess possible source confusion situations. We also obtained and analyzed archival XMM/MOS data for the NGC 1313 source, and Chandra and XMM archive data for the M82 ultraluminous source. In the case of NGC 1313, the observations with XMM were made during an apparent low-hard state of that source, thus making it difficult to deconvolve the thermal and Comptonized components, so we did not use these data in our final analysis. The results presented for that source are based on one of two archived ASCA observations, when a high-soft-state spectral form was exhibited. Similarly, we were unable to interpret the spectrum that we derived for the M82 source in the context of our model (or any obvious thermal plus Comptonization model, although see Strohmayer & Mushotzky 2003), thus we did not include that object.

We performed forward-folding spectral analysis applying the bulk-motion Comptonization model to obtain the normalization parameter described in Section 2, and in BOR99 and ShT99. The similarity between the BHXRBs, NLS1s and ULXs is evidenced in Figure 2; here familiar HSS BHXRB spectral form is mimicked by the other representative objects (although the NLS1 characteristic temperature is much lower).

3.1. Galactic BHXRBs

We have applied our analysis to a sample of 13 Galactic BHXRBs, as indicated in Table 1; also see to Figure 3. As noted, we have used GRO J1655-40 as our primary calibrator, with additional self-consistency checks such as GRS 1915+105, XTE J1859+226 and XTE J1550-56. The accuracy of the distance estimates vary considerably over our sample, and this is a major component to the uncertainty in our mass determination; as noted we are really computing the mass-to-distance ratio. We have thus included a distance column in Table 1 with numbers drawn from the recent literature, indicating the value used in our calculation.

The most notable discrepancy between our results, and those tabulated in Orosz (2002; also see Shahbaz, Naylor & Charles 1997) for Nova Muscae 1991 and LMC X-1. For Nova Muscae 1991, our mass estimate of 12.5 ± 1.6 exceeds the dynamical mass by about 2.5σ . Also for LMC X-1, which is poorly constrained dynamically, our result is about 1σ above the upper bound in Orosz (2002).

We made a self-consistency check by estimating the mass accretion rate in the disk \dot{m}_{disk} in cases where the the distance and thus mass are known. We remind the reader that $\dot{m}_{disk} = \dot{M}/\dot{M}_E$ where $\dot{M}_E = L_E/c^2$ and $L_E = 4\pi GMm_p/\sigma_T c$. We then applied the formula for \dot{m}_{disk} inferred in BOR99 (see eq. 8 of that reference). We note that Chakrabarti & Titarchuk (1995) argued that \dot{m}_{disk} should be of order of unity or higher in the high/soft state. One can also calculate the luminosity of the soft component, L_s , using formula (9) in BOR99 once m and \dot{m} are determined. *For all Galactic and extragalactic BH sources that we have analyzed, we find that the high-soft condition $\dot{m}_{disk} \gtrsim 1$ is satisfied and $L_s < L_E$ (in most cases L_s is a few percent of L_E).*

3.2. Narrow-Line Seyfert-1 Galaxies

The narrow-line Seyfert-1 Galactic Nuclei (NLS1s) are another class of objects to which our technique can be applied. These objects, summarized in detail in elsewhere (e.g. Leighly 1999a; 1999b; Vaughan et al 1999), are found to have an excess of soft X-ray emission relative to a powerlaw component, which is in turn softer (photon indices $\Gamma \simeq 2 - 2.5$, as opposed to $1.7 - 1.8$) than that of the broader class of Seyfert-1 galactic nuclei. As has been noted, their spectra often resemble those of Galactic black-hole X-ray binaries in the high-soft state (Figure 2). Implicit in our analysis is the assumption that the soft-excess, as in the Galactic binaries, associated with high mass-accretion rates.

There have been suggestions that the masses of the central compact objects in the NLS1s may be systematically lower, perhaps by as much as a factor ~ 10 than those of

typical broad-line Seyfert galactic nuclei. One possible explanation is that the black holes in these systems are still being grown, and thus the copious soft X-rays. However, this may be an overly simplistic an argument, and the empirical picture needs to be further solidified.

In a number of cases, independent estimates are available from reverberation mapping and/or bulge mass/velocity dispersion correlations (e.g. Wandel, Peterson & Malkan 1999) methods, so a direct cross-comparison of our results to those methods can be made. More recently, cross-calibration of those methods with observational properties which are more easily obtained, such as bulge magnitude or narrow emission-line properties. This has led to much more extensive compilations (e.g. Woo & Urry 2002). From these tabulation in the literature, we can compare our results as a cross check, and to see if any systematic trends are evident.

To further explore these issues, we have revisited observational data for a subset of the NLS1 population. We have applied our fitting procedure, as described above, to the NLS1 sample listed in Table 2. From the parameters enumerated in Table 2, using the luminosity distances determined from the known source redshifts, we can then estimate the central BH mass following the procedures outlined in section 2.

Generally, the functional form of the model fits resemble the Galactic black-hole X-ray binary high-soft-state. The characteristic blackbody temperatures however, are typically lower, $kT \simeq 0.1$ keV. We have studied the issue of the color factor determination for these lower temperature environments. This issue has been previously addressed in radiative transfer calculations in accretion disks of super-massive objects (Hubeny et al. 2001, hereafter HBKA). The analytic and numerical radiative transfer models in HBKA are reasonably self consistent and are, in principle, able to produce high-temperature external layers, the so called “disk corona”. Comptonization in these corona leads to an increase in the color factor T_h dependent upon a model parameter of the disk, ϵ known as the ‘mean photon destruction parameter’. T_h can vary from 2 to 40 as ϵ changes from 10^{-2} to 10^{-8} . Such a wide range possible of T_h values does not allow us to specify a certain value of T_h using the HBKA disk model but it demonstrates that high values of T_h may not be excluded. We found that the our set of mass estimates for supermassive objects would be agree reasonably well with those derived from other methods if $T_h \simeq 12$. Our results are depicted graphically in Figure 4.

3.3. ULXs

Another class of objects which have been seen to exhibit the high-soft/low- hard state bimodality are the ultra-luminous X-rays sources (ULXs) seen in a number of nearby galaxies,

notably in or near star forming regions (e.g. Ptak & Colbert 2002). Ultra-luminous in this context refers to apparent luminosities in the $\simeq 1 - 10$ -keV X-ray band of $\sim 1.5 \times 10^{38}$ erg s $^{-1}$, which is well in excess of the Eddington limit for solar mass objects (Colbert & Mushotzky (1999); Griffiths et al. 2000; Kaaret et al. 2001). Furthermore, the spatial resolution of the Chandra X-ray Observatory has demonstrated that in a number of cases, such objects are clearly distinct from the dynamical center of the host Galaxy. This in particular has generated considerable interest, as one possible explanation which avoids the Eddington-limit problem is that objects of "intermediate" mass scale, $\simeq 10^2 - 10^4 M_{\odot}$ are present in interacting binaries. Alternative hypotheses, invoking beaming have also been suggested to avoid this problem (King et al 2001), but this may be problematic, as at least some objects apparently illuminate reflection nebulae. Also, the spectral energy distribution in at least some cases has a distinctly thermal component, and perhaps most significantly, the recent discovery of quasi-periodic oscillations in the M82 source argue very strongly for a compact disk-fed system, quite likely a binary (Strohmayer & Mushotzky 2003). We thus suggest that this is a pertinent area of investigation for alternative mass-estimation methods. We note that this has already been calculated using the ShT99 technique in a preliminary manner and presented in Colbert & Mushotzky (1999) .

We should also note that there are instances of Galactic or Megallanic cloud X-ray binaries which have exhibited luminosities overlapping the lower extent of the nominal ULX luminosity distribution (e.g. McClintock & Remillard 2003). We attempt to address this in section 4.

We have applied our model fitting and mass determination procedure to 7 objects in 6 galaxies categorized as ULXs. Each are previously noted in the literature to exhibit an apparent thermal excess plus unsaturated Comptonization spectrum; (NGC 1313, NGC 5408 & M33: Colbert & Mushotzky 1999; NGC 253, NGC 1399 X-2, NGC 1399 X-4; Humphrey et al 2003). Results are presented in Table 3 (also see Figure 6). The most compelling cases for the presence of intermediate mass objects are for the NGC 1313 and NGC 5408 objects. Our calculations for the NGC 253 source, and the two NGC 1399 sources also suggest objects of intermediate mass in the $10^3 - 10^4$ range, however, we consider these results less certain. These sources are faint, and the spectra we were able to extract consist of only 500-1000 net photons. This is reflected in the size of the error bars associated with those sources in Figure 5, which is ultimately due to our inability to better constrain the kT and normalization parameters of our spectral deconvolution.

Our results the M33 source however, are consistent with it being a few ~ 10 solar mass object, perhaps not entirely dissimilar from GRS 1915+105. As noted, we were unable to obtain useful results in the context of our methodology for the M82 source, or for the

apparent low-hard-state situations in the NGC 1313 observations of July 12, 1993 (ASCA) or October 17, 2000 (XMM). The shortcoming in each of these instances was our inability to reliably extract a thermal component.

4. Discussion and Conclusions

To summarize: (i) we have presented a method for the determination of central black-hole masses based on X-ray spectral extraction (ii) the principal parameter of the method, the X-ray color factor has been established empirically for BHXRBs and NLS1 subclasses (iii) the NLS1 mass distribution we find is offset from the distribution of normal Seyfert-1 mass estimates. In small overlap between our sample and published mass estimates from reverberation mapping, there is good agreement in one case (Mkn 110), poor agreement in ones case (NGC 4051), and nominal agreement in another (Mkn 335). (iv) The results we obtain for NGC 1313, NGC 5408, NGC 253, NGC 1399 are consistent with the existence of intermediate mass objects in those systems, specifically black hole masses of ~ 170 , ~ 110 , $\sim 10^3$ and 3.5×10^3 solar masses respectively. For the M33 source, the our mass estimate suggests an ~ 30 solar mass object, so it may be an extreme manifestation of a supernova produced stellar mass black hole. (v.) Our inferred estimates of luminosity using the best-fit parameter T_{col} , and inferred BH masses [see equation (9) in BOR99, for details] show that for the most of the analyzed sources the bolometric luminosity in the high/soft state is a few percents of the critical (Eddington) luminosity.

There are some instances in the literature where other authors have cited difficulty in reconciling the observed temperatures with intermediate BH masses (see e.g. Kubota et al. 2002). We revisited some of those same data within the context of our own analysis, notably for the IC 342 "source 1", which was the basis of Kubota et al. (2002) paper. We find that our Comptonization model (BMC) provides a good fit ($\chi^2=268/266$) with parameters $T = 0.11 \pm 0.07$, keV and spectral index $\alpha = 0.61 \pm 0.05$, typical a for low/hard state accreting black hole. No additional components were required to obtain a reasonable spectral fit. The inferred temperature T and the normalization of the blackbody component A_n allow us to estimate the BH mass for this source. The value we obtain is of order of 4×10^3 solar masses (see Table 3). As previously noted in Titarchuk & Shrader (2002) (see also Merloni, Fabian & Ross 2002), typically, problems with the interpretation of X-ray spectral data are driven either by the application of an additive, phenomenological model of the spectrum or by the models related to the determination of the inner disk temperature and radius. One must bear in mind that the temperature of the inner disk radius is not an observable quantity, rather it is a inferred parameter of this particular disk model. The contribution to the spectrum of the

innermost region can be significantly overestimated as a result of approximating the inner boundary conditions. A self-consistent analysis of the disk emission area, in the case when the entire disk is exposed to the observer, reveals that it exceeds the inner-most area by an order of magnitude. In practical terms, this means that there is little spectral information on this region.

There are interpretations (Mukai et al 2003, Fabbiano et al, 2003) which invoke an optically thick outflow from Eddington-limit accretors, for which the observed luminosities are compatible with stellar-mass central objects. Thus, one might pose the question: is it the two different assumptions about the origin of the soft component that lead to the different masses? In fact, the spectrum by itself does not provide the information on geometrical configuration of the emission area (see Titarchuk & Lyubarskij 1995). One needs timing characteristics (QPOs, time lags, the power spectrum as a function energy) in order to reveal the geometrical configuration. In our analysis we were guided by the similarity of the high/soft states in ULX to BHXRBs in which the presence of the high frequency QPOs is well established. In this sense we assume the soft component originates in the disk but not in “an optically thick outflow”. Recent findings of “high frequency” QPOs by Strohmayer & Mushotzky (2003) provide a very strong basis for our assumption. Indeed, the assumption that the disk radiation is the origin of the soft component plus the self-consistent procedure for the mass evaluation and comparison of our results to other methods support the validation of our approach.

One can argue on the fact that there are a number of perfectly normal stellar-mass X-ray binaries have luminosities overlapping the ULX regime; see for example section 4.2.4 of the recent comprehensive review of black hole observations by McClintock and Remillard (2003). In the McClintock & Remillard (2003) review, they note in particular, three examples of over-luminous BHXRBs: 4U 1453-47, V404 Cyg and V4641 Sgr. We have included 4U 1453-47 and V4641 Sgr in our analysis, however, the data used for V4641 Sgr were not obtained during the apparent 1999 super-Eddington event (those data were all obtained with RXTE in a scanning configuration, which along with possible saturation issues leads to analysis difficulties). Also, since the spectrum is in , or transitioning to the low-hard state, we made the assumption that the inner-disk radius had receded to $17 R_s$ (see ST99). For 4U 1543-47, the analysis presented is based on RXTE observations of June 21, 2003, at which time the source luminosity was about $2 \times 10^{38} \text{ ergs/cm}^2/\text{s}$ assuming a distance of 6.4 kpc. In both cases, our results are consistent with those objects being stellar-mass black holes. The 1989 outburst of V404 Cyg was covered by GINGA, however, the high-level data products available from the HEASARC cover only several epochs of the late decay stage, several months after the May/June 1989 peak. More fundamentally, the peak luminosities exhibited by these sources are aperiodic intensity surges of relatively short duration, rather

than the stable disk accretion scenarios that comprise the basis of our study.

Merloni, Fabian & Ross (2000) stress that disk inclination is a concern, as a rigorous treatment must consider Doppler boosting effects, which can modify the emergent spectrum, particularly at high energies. In principle this problem can be solved in the framework of a disk model with an assumption regarding distribution of energy release over the disk. In practice however, one would need to know the disk equation of state, and then calculate the spectrum at each annulus, taking into account not only Doppler boosting effects, but the warping of the disk as well. In our view, there are simply too many uncertainties inherent in this approach. Rather, we argue that some effects of the Doppler boosting and disk warping can be implicitly present in the data through the spectral hardening factor T_h . Possibly it is not by chance $T_h = 2.6$ is relatively high in all these BHs. The detailed study of this issue is beyond the scope of this paper.

We note that we have not considered the case of rapidly rotating black holes. Several objects among our sample, notably GRO J1655-40 and GRS 1915+105 have been cited as possible examples of extreme Kerr black holes on the basis of the detection of high-frequency QPOs (e.g. Strohmayer 2001; McClintock & Remillard 2003 and references therein), and XTE 1650-500 has been identified by Miller et al (2003) as a candidate rapidly-rotating object on the basis of spectroscopic analysis. However, we note that there are concerns regarding the interpretation of the QPOs, notably the apparent synergy between BH, NS and WD systems (Mauche 2002), which argues against models invoking general relativistic effects. Furthermore, alternative explanations have been put forth (e.g. Titarchuk & Wood 2002, Titarchuk 2003). Additionally, we find no evidence in our own spectral analysis for the presence excess emission in the 4-6 keV region, although we are working with the coarse RXTE spectral resolution. We would further note that alternative explanations of those features has recently emerged (Titarchuk, Kazanas & Becker 2003). Thus, while we acknowledge that, if corroborated by further study, the presence of rapidly rotating objects could alter our conclusions for some cases, we suggest that the issue is unresolved.

Our mass-distribution results for the NLS1s, namely that the distribution is shifted towards lower values relative to other AGN, is consistent with the hypothesis that they may represent an early, evolutionary stage of the broader AGN class, in which the central black hole is still undergoing growth through interaction with bulge material. If this is the case, one might speculate that a larger fraction of soft-excess AGN may be seen with increasing redshift. This is consistent at least with results on the spatial variance statistics for the soft/hard subsamples of the deep surveys, but nonetheless remains speculative.

ACKNOWLEDGMENTS

This work made use of the High-Energy Astrophysics Science Archive Research Center at the NASA Goddard Space Flight Center, as well as the NASA Extragalactic Database (NED) at the NASA Jet Propulsion Laboratory. We appreciate very interesting questions and suggestions of the referee.

REFERENCES

- Borozdin, K., Revnivtsev, M., Trudolyubov, S., Shrader, C.R., & Titarchuk, L.G. 1999, ApJ, 517, tbd. (BOR99)
- Chakrabarti, S.K., & Titarchuk, L.G. 1995, ApJ, 455, 623
- Colbert, E., & Mushotzky, R. 1999, ApJ, 519, 89
- Fabbiano, G., Elvis, M., Markoff, S., Siemiginowska, A., Pellegrini, S., Zezas, A., Nicastro, F., Trinchieri, G., McDowell, J. 2003, ApJ, 588, 175
- Ferrarese, L., Merrit, D. 2000, ApJ, 539, L9
- Greiner, J., Cuby, J., & McCaughrean, M.J. 2001, Nature, 414, 522
- Griffiths, R.E. et al. 2000, Science, 290, 1325
- Grimm, H.-J., Gilfanov, M. & Sunyaev, R. 2003, MNRAS, 339, 793
- Hubeny, I., Blaes, O., Krolik, J.H., & Agol, E. 2001, ApJ., 559, 680
- Humphrey, P.J., Fabbiano, G., Elvis, M., Church, M.J., & Balucinska-Church, M. 2003, MNRAS, (in press) (astro-ph/0305345)
- Kaaret, P., et al. 2001, MNRAS, 321, L29
- King, A.R., Davies, M.B., Ward, M.J., Fabbiano, G., & Elvis, M. 2001, ApJ, 552, L109
- Kubota, A., Done, C., & Makishima, K. 2002, MNRAS, 337, 11
- Leighly, K. 1999, ApJS, 125, 317
- McClintock, J. & Remillard, R. (2003) (astro-ph/0306213)
- Mathur, S. 2001, New Astr, 6, 321
- Mauche, C. W., 2002, ApJ, 580, 423
- Merloni, A., Fabian, A.C., & Ross, R.R. 2000, MNRAS, 313, 193
- Miller, J.,M., Fabbiano, G., Miller, M.C., & Fabian, A.C. 2003, ApJ, 585, L37
- Mukai, K., Pence, W. D., Snowden, S. L., Kuntz, K. D. 2003, ApJ., 582, 184

- Novikov, I.D., & Thorne K. 1972, In Black Holes, (De Witt and B.S. De Witt (eds.) New York:Gordon and Breach, 1972, p. 935
- Orosz, J.A., Bailyn, C.D. 1997, ApJ, 477, 876
- Orosz, J., et al. 2002, in” A Massive Star Odyssey, from Main Sequence to Supernova”, IAU Symp. 212, eds. K. A. van der Hucht, A. Herraro, & C. Esteban, (San Francisco: ASP), in press (astro-ph/0209041)
- Ptak, A., & Colbert, E. 2002, ApJS, 143, 25
- Shahbaz, T., Naylor, T., & Charles, P.A. 1997, MNRAS, 285, 607
- Shakura, N.I., & Sunyaev, R.A. 1973, A&A, 24, 337 (SS73)
- Shimura, T., & Takahara, F. 1995, ApJ, 445, 780
- Shimura, T., & Takahara, F. 1995, ApJ, 445, 780
- Shrader, C.R., & Titarchuk, L.G. 1999, ApJ, 521, L121 (ShT99)
- Strohmayer, T.E. 2001, ApJ, 552, L49
- Strohmayer, T.E., & Mushotzky, R.F. 2003, ApJ, 586, L61
- Sunyaev, R.A. & Titarchuk, L.G. 1973, A&A, 86, 121
- Titarchuk, L.G. 1994, 429, 340 (Ti94)
- Titarchuk, L., Kazanas, D. & Becker, P.A. 2003, ApJ, in press
- Titarchuk, L.G. & Lyubarskij, Yu. 1995, ApJ, 456, 876
- Titarchuk, L. G., Mastichiadis, A., & Kylafis, N. D. 1997, ApJ, 487, 834 (TMK97)
- Titarchuk, L. G., & Shrader, C.R. 2002, ApJ, 567, 1057
- Titarchuk, L.G. & Zannias, T. 1998, 493, 863
- Vaughn, S., Reeves, J., Warwick, R., & Edelson, R. 1999, MNRAS, 309,113
- Woo, J-H, & Urry, C.M. 20002, ApJ, 579, 530.
- Wandel, A., Peterson, B.M., & Malkan, M.A. 1999, ApJ, 526, 579

Table 1. Galactic BHXRBs

Source ID	α	kT (keV)	d_{kpc}	M_i^a
GRS 1758-258	1.47 ± 0.03	0.30 ± 0.04	8.5	5.7 ± 1.7
GX 339-4	1.31 ± 0.14	0.85 ± 0.06	4	9.0 ± 3.8
XTEJ1550-564	1.55 ± 0.03	0.86 ± 0.02	5	9.4 ± 2.1
XTE J1650-500	1.21 ± 0.03	0.61 ± 0.08	5	10.6 ± 4.0
LMC X-1	1.63 ± 0.03	0.79 ± 0.06	55	11.2 ± 1.5
Nova Muscae	1.36 ± 0.04	0.86 ± 0.07	4	12.5 ± 1.6
GRS 1915+105	1.7 ± 0.10	0.90 ± 0.08	11	13.3 ± 4.0
4U 1630-47	1.43 ± 0.02	0.95 ± 0.02	10	7.4 ± 1.5
XTE J1859-224	1.74 ± 0.02	0.82 ± 0.08	11	12.3 ± 1.7
4U 1547-43	1.43 ± 0.01	0.75 ± 0.01	6.4	14.8 ± 1.6
EXO 1846-031	1.88 ± 0.07	0.75 ± 0.07	6	12 ± 5
XTE J1755-32	1.10 ± 0.04	0.66 ± 0.01	8	8.4 ± 4
GRS 1739-278	1.58 ± 0.06	0.92 ± 0.09	8	7.7 ± 4
V4641 Sgr	1.97 ± 0.10	0.32 ± 0.029	9.5	7.5 ± 2

$$^a M_i = M(\cos i)^{1/2}$$

Table 2. Narrow Line Seyfert-1 Galaxies

Source ID	α	kT (keV)	z	$\log M_i^a$
Ark 564	1.48 \pm 0.01	0.16 \pm 0.01	0.024	6.31 \pm 0.02
H0707-495	1.26 \pm 0.08	0.10 \pm 0.00	0.040	6.72 \pm 0.00
IRAS17020 4544	1.18 \pm 0.03	0.22 \pm 0.01	0.060	6.01 \pm 0.04
IRAS20181-224	1.28 \pm 0.13	0.25 \pm 0.03	0.185	5.96 \pm 0.08
IZw1	1.19 \pm 0.05	0.19 \pm 0.02	0.061	5.99 \pm 0.08
Mkn335	0.90 \pm 0.03	0.16 \pm 0.01	0.026	6.01 \pm 0.06
Mkn42	0.82 \pm 0.11	0.20 \pm 0.02	0.024	5.31 \pm 0.07
NAB 0205 024	1.17 \pm 0.04	0.16 \pm 0.01	0.155	6.62 \pm 0.05
NGC4051	0.93 \pm 0.01	0.09 \pm 0.00	0.002	5.89 \pm 0.00
PG1211 143	1.01 \pm 0.03	0.11 \pm 0.01	0.080	6.83 \pm 0.05
RE J1034 39	1.14 \pm 0.11	0.13 \pm 0.01	0.042	6.26 \pm 0.04
RX J0148-27	0.98 \pm 0.10	0.12 \pm 0.02	0.121	6.77 \pm 0.10
Mkn110	0.83 \pm 0.09	0.11 \pm 0.01	0.036	6.79 \pm 0.03
PKS 0558-504	1.02 \pm 0.06	0.26 \pm 0.03	0.137	6.79 \pm 0.05
Mkn766	0.87 \pm 0.02	0.08 \pm 0.00	0.012	6.09 \pm 0.04
Ton S180	1.34 \pm 0.03	0.17 \pm 0.00	0.062	6.38 \pm 0.02
PHL 1181	1.3 \pm 0.7	0.086 \pm 0.027	0.190	7.01 \pm 0.3

$$^a M_i = M(\cos i)^{1/2}$$

Table 3. Ultra-Luminous non-Nuclear Extragalactic X-Ray Sources

Source ID	<i>R.A.</i>	<i>Dec</i>	<i>kT</i> (keV)	α	<i>d_{kpc}</i>	$\log(M_i)^a$
M33	01 33 51.1	+30 39 37	0.39± 0.01	1.41± 0.06	700	1.46± 0.19
NGC 1313	03 18 20.3	-66 29 11	0.28± 0.06	1.31± 0.02	3700	2.22± 0.05
NGC 5408	14 03 19.4	-42 22 58	0.11± 0.01	1.20± 0.10	4900	2.03± 0.05
NGC 253	00 47 17.6	-25 18 11	0.12 ± 0.03	1.1±0.24	3100	3.01± 0.13
NGC 1399 X-2	03 38 31.8	-35 26 04	0.102 ± 0.022	2.18± 0.43	20000	3.54± 0.16
NGC 1399 X-4	03 38 27.6	-35 26 48	0.15 ± 0.08	2.5± 1.4	20000	3.34± 0.22
IC 342 X-1	03 45 59	68 05 05	0.11 ± 0.01	0.62± 0.05	4000	3.63± 0.30

$$^a M_i = M(\cos i)^{1/2}$$

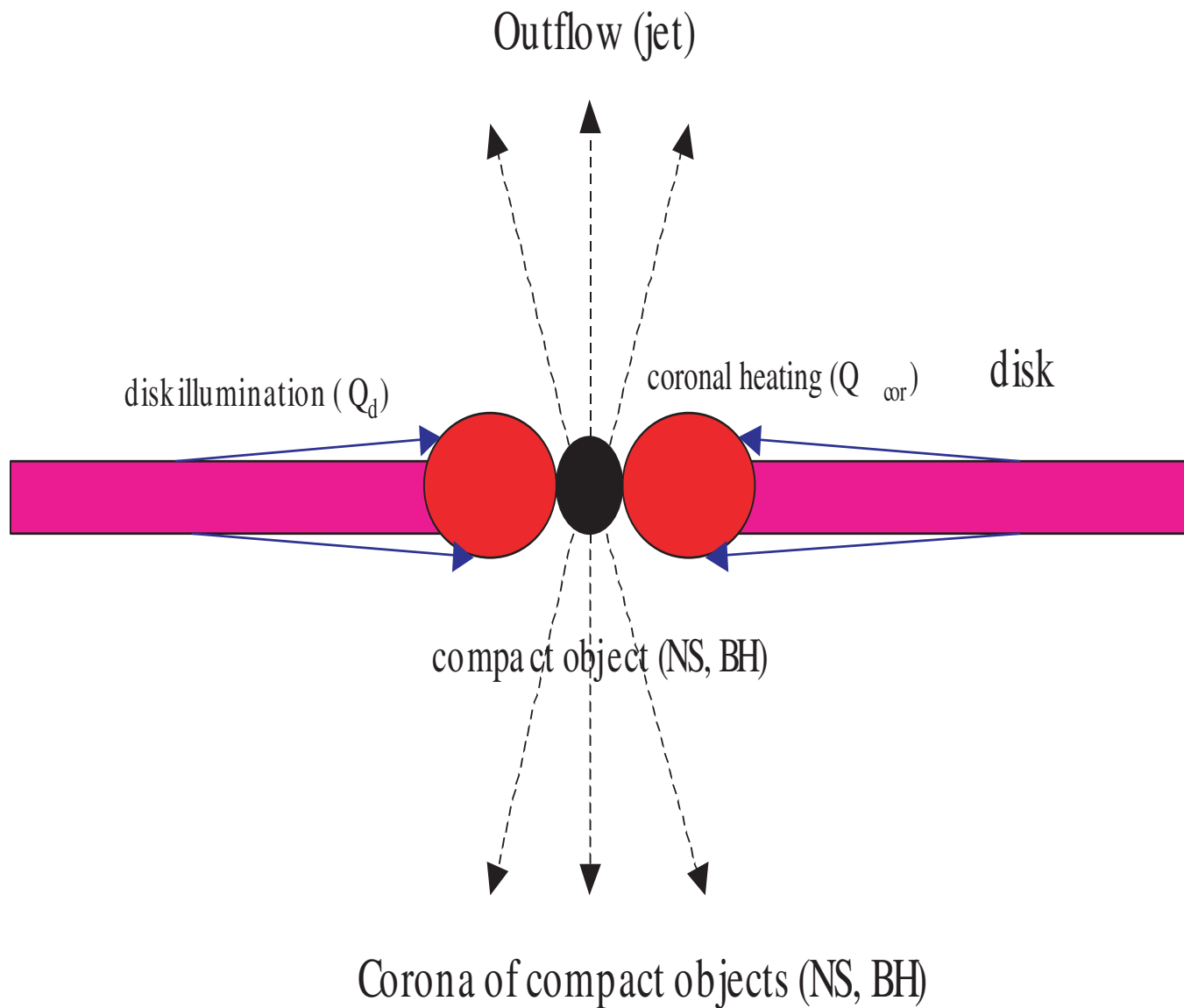


Fig. 1.— Artist’s conception of our model. The low-energy blackbody X-ray photons are assumed to come directly from the thin accretion disk. The higher energy photons that form the power law tail of the spectrum come from upscattering (acceleration) by energetic electrons depicted in circular regions internal to the disk. Some fraction of the disk photons are viewed directly, while another fraction are seen after scattering in the coronal region.

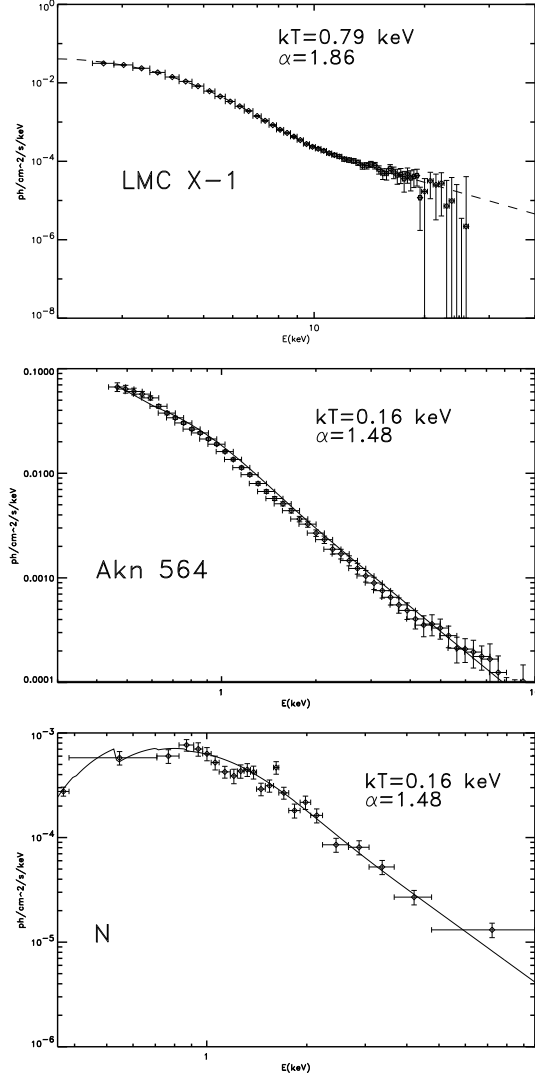


Fig. 2.— Representative spectral energy distributions for a BHXRB (LMC X-1), a NLS1 (Akn 564), and an ULX (NGC 1313). Plotted are the data, corrected for the instrumental response (points), and the model as described in the text. Note that the basic power-law plus soft-excess form is a common feature, although the characteristic black-body temperatures kT differ ($\sim 1 \text{ keV}$, $\sim 0.5 \text{ keV}$, and $\sim 0.2 \text{ keV}$ for LMC X-1, NLS1 and NGC 1313 respectively). Note that α is the energy flux spectral index.

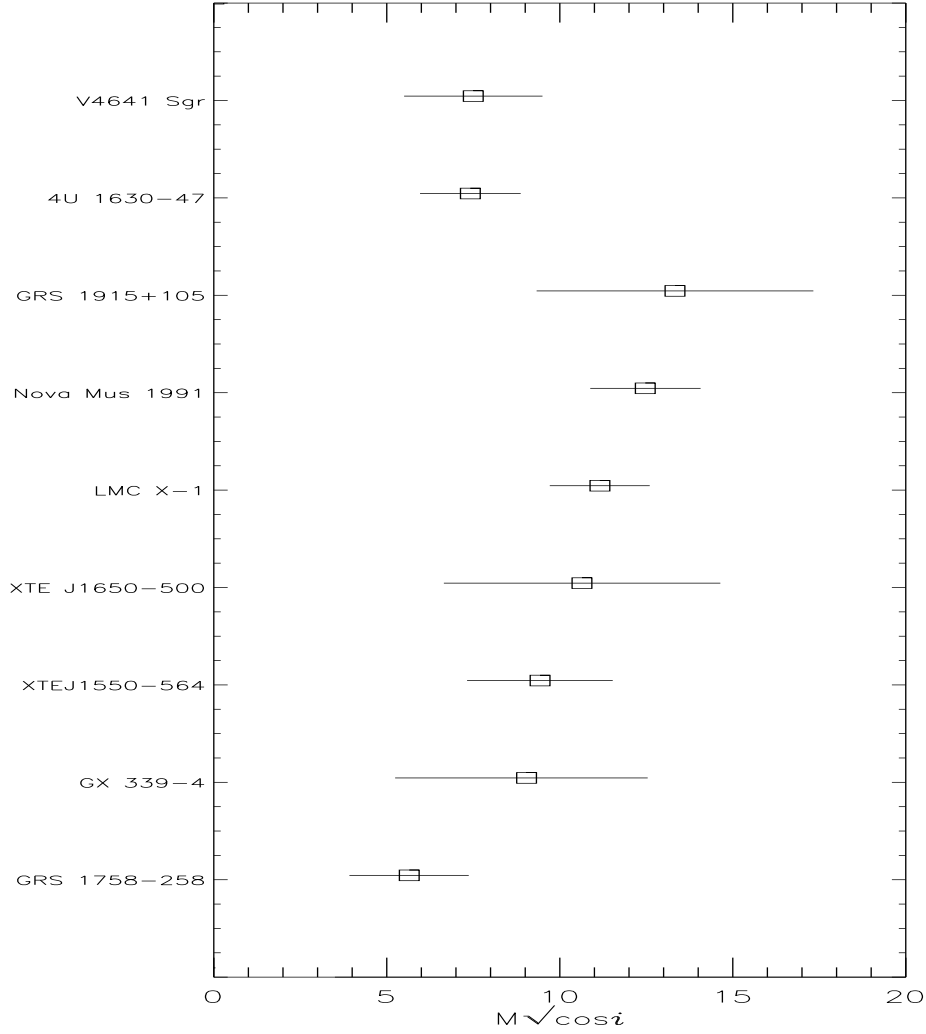


Fig. 3.— The horizontal axis in this case is $M_i = M_{BH} \cos i$ in solar units, while the vertical axis delineates between objects. Other than Nova Muscae 1991, and possibly LMC X-1 (but see ShT99), our results are in reasonable agreement with dynamical mass determinations where such measurements are available.

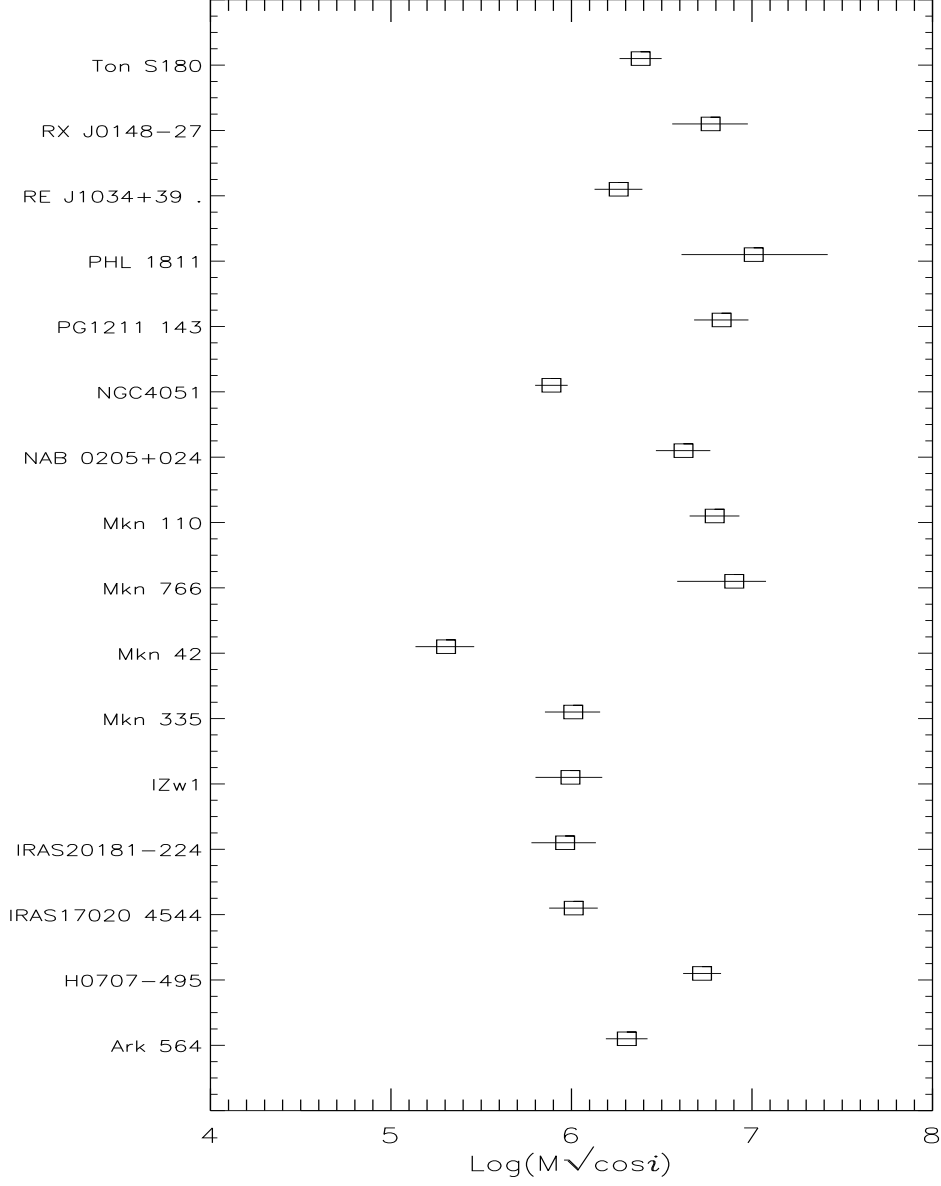


Fig. 4.— Distribution of our mass-determination results for our NLS1s sample. The horizontal axis in this case is $\text{Log}(M_i)$, while the vertical axis delineates between objects. $M_i = M_{BH} \cos i$ in solar units. The error-bars represent the uncertainties associated with the color factor, which as noted in the text can vary over a wide range for AGN disks.

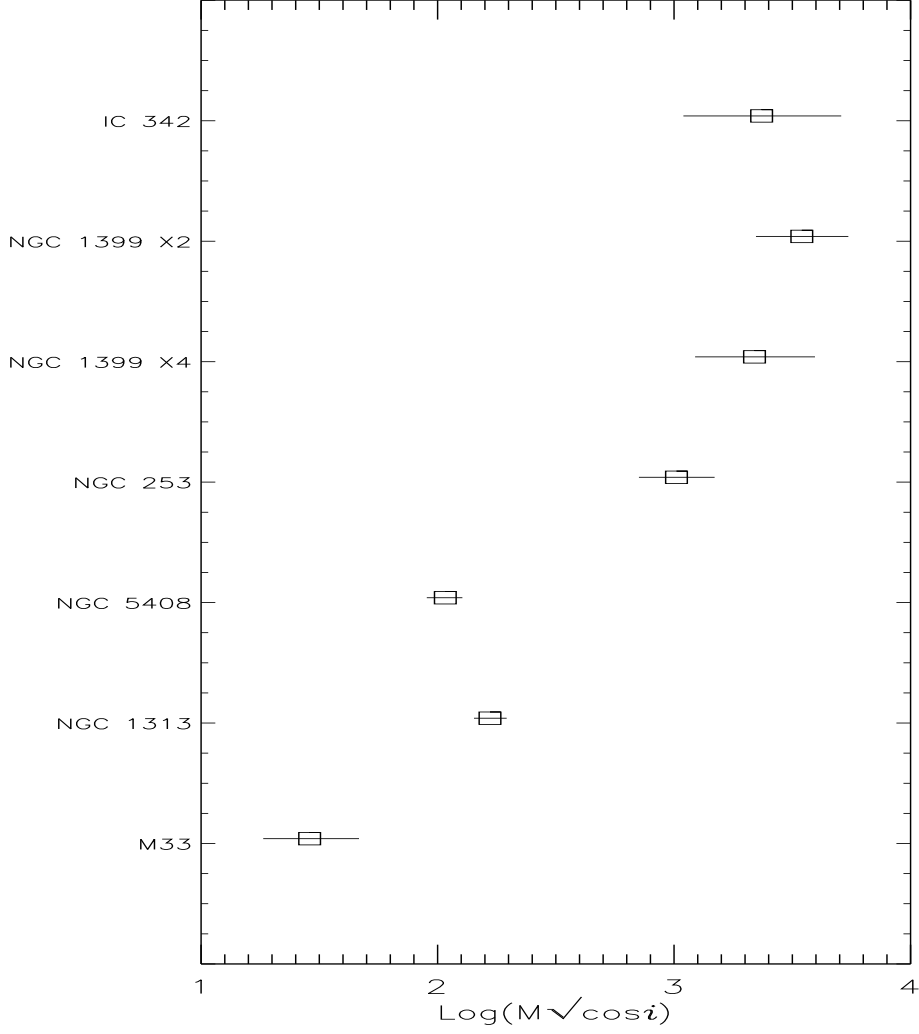


Fig. 5.— Mass-determination results for three well known extragalactic over-luminous non-nuclear X-ray source sample. The horizontal axis in this case is $\text{Log}(M_i)$, while the vertical axis simply delineates between objects. $M_i = M_{BH} \cos i$ in solar units. The error-bars, again represent essentially the uncertainties associated the color factors.

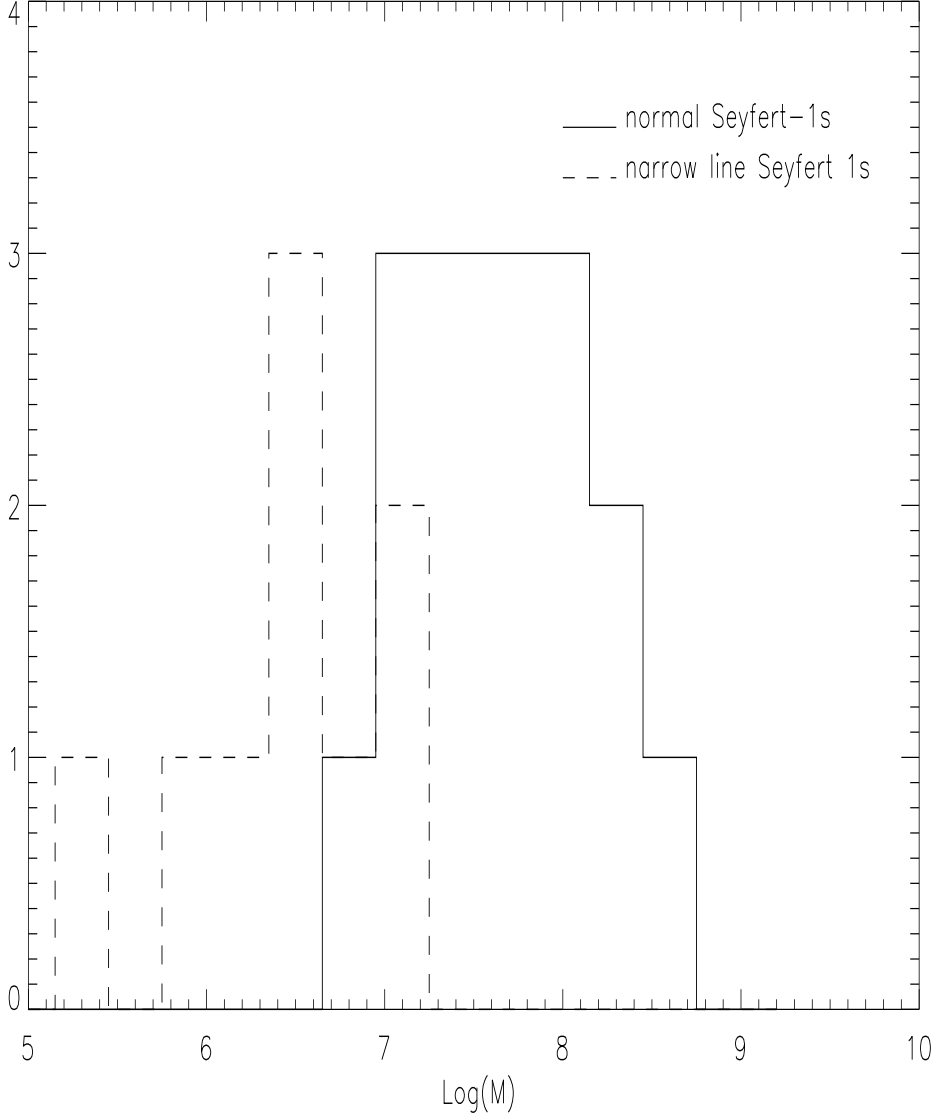


Fig. 6.— Distribution of our NLS1 BH mass estimations. For comparison, a sample of normal Seyfert-1 nuclear BH mass estimates from the literature (Woo & Urry, 2002) are shown as well. Our results suggest, in the absence of some unforeseen systematic error in our analysis, that the NLS1 population comprise a lower-mass Seyfert sub-population.